Fingerprints of viscoelastic subdiffusion in random environments: Revisiting some experimental data and their interpretations

Igor Goychuk [*] and Thorsten Pöschel

Institute for Multiscale Simulation, Department of Chemical and Biological Engineering, Friedrich-Alexander University of Erlangen-Nürnberg, Cauerstr. 3, 91058 Erlangen, Germany

Many experimental studies revealed subdiffusion of various nanoparticles in diverse polymer and colloidal solutions, cytosol and plasma membrane of biological cells, which are viscoelastic and, at the same time, highly inhomogeneous randomly fluctuating environments. The observed subdiffusion often combines features of ergodic fractional Brownian motion (reflecting viscoelasticity) and nonergodic jumplike non-Markovian diffusional processes (reflecting disorder). Accordingly, several theories were proposed to explain puzzling experimental findings. Below we show that some of the significant and profound published experimental results are better rationalized within the viscoelastic subdiffusion approach in random environments, which is based on generalized Langevin dynamics in random potentials, than some earlier proposed theories.

I. INTRODUCTION

Brownian motion is omnipresent and important in physics providing a paradigm in soft matter and biological physics [1]. It is generally characterized by a linear in time spread of the particle positions' variance, $\langle \delta x^2(t) \rangle \propto t^\alpha$, on the ensemble level of description, with $\alpha = 1$, which is the case of normal diffusion in the contemporary phrasing. However, anomalous diffusion with other scaling power-law exponents $0 < \alpha < 1$ (subdiffusion) and $\alpha > 1$ (superdiffusion) became increasingly popular over the last 50 years [2–4]. Also another important, logarithmic scaling in subdiffusion with $\langle \delta x^2(t) \rangle \propto |\ln t|^a$ with $a > 0$ can be met in nature [2–4]. Nominally it is named ultraslow diffusion with the particular exponent $a = 4$ corresponding to the so-called Sinai diffusion [2–5]. This "ultraslow" can, however, be a quite misleading naming [6,7]. Also, normal, according to the $\alpha = 1$ criterion, diffusion can be anomalous concerning the probability density $P(x, t)$ of the particle positions' spread. Indeed, instead of Gaussian or normal distribution, the Laplace or exponential distribution was revealed experimentally in several studies and named anomalous, yet Brownian diffusion [8,9].

There are many different theories [2–4,10,11] aimed to rationalize anomalous diffusion. Various physical systems may require quite different theoretical approaches. In this paper, we are dealing with soft matter liquidlike systems, where the approaches of viscoelastic subdiffusion [10,11] seem most appropriate. Indeed, soft media such as dense polymer solutions, cytosol of biological cells, biological membranes, and even interface layers of water are intrinsically viscoelastic [12–19]. In living cells, the underlying random polymer network consisting, in particular, of actin and other biopolymer filaments [20,21] provides a natural physical environment for various mobile nano- and microparticles. The microrheological properties of such a medium can be characterized by a complex

shear modulus [12–14], $G^*(\omega) = G'(\omega) + iG''(\omega)$, with elastic, $G'(\omega)$, and loss, $G''(\omega)$, parts. They both often show a power-law scaling, $G'(\omega), G''(\omega) \propto \omega^\beta$, in certain frequency range(s), with some power-law exponent β, which often corresponds to the power-law exponent of anomalous diffusion, $\beta = \alpha$ [12–14]. For example, actin filament solutions are macroscopically characterized by $\beta = \alpha = 0.75$ [12,14,21].

Such viscoelastic media can be considered as soft glassy materials (SGMs) [21,22], which can phenomenologically be characterized by a dimensionless noise temperature x in accordance with a random medium theory proposed in [22]. Above the temperature of glass transition at $x = 1$ and for the range $1 < x < 2$, $\beta = x - 1$ [22]. Then, the medium should be ergodic and fluidlike [22]. For example, microrheology of some living cells yielded $\beta \sim 0.15$–0.35 [23] in a low-frequency range, which was interpreted as $x \sim 1.15$–1.35 within the SGM model. Other cells can exhibit other β. For example, $\beta = 0.4$ or 0.5 in [24] depending on whether microtubuli are present or not. Sometimes the corresponding microrheology, which is characteristic for living cells, is named power-law microrheology [21].

The actin networks can, however, also display experimentally β less than 0.75 at small frequencies [21], which was explained within a glassy wormlike chain (GWLC) model [21,25,26]. The GWLC model, like the SGM model, is essentially based on a random barrier assumption typical for random media. The larger the disorder, the smaller is β [21,25,26]. These two models are important. However, they cannot explain all the facts of anomalous diffusion in polymer networks, which are porous and can be characterized by a random mesh size. Here, the ratio of the particle size to the mesh size becomes an important parameter and α can be very different from β [27–29].

Transport processes in cytosol and plasma membrane are vital for living cells [20,30]. A number of experimental studies [15,16,30–40] revealed their anomalous subdiffusive character. It is generally believed that subdiffusion of various

_____
[*]igor.goychuk@fau.de

nano- and submicron particles in such inhomogeneous crowded media is essentially based on viscoelasticity. Typical power-law anticorrelations of the test particle displacements often follow the pattern of a fractional Brownian motion (FBM) [41], in agreement with a theory based on generalized Langevin equations (GLEs) [10,13,14]. However, such media are also featured by intrinsic randomness, which is, e.g., a central part of the SGM and GWLC models [21] and can also manifestly influence diffusion and transport processes. Randomness is fundamental for the continuous-time random walk (CTRW) description of subdiffusion [3,4,42–44], where the particles sojourn for a long random time in some trapping domain and relatively fast change their location to a different trap. Here, the approach based on infinite mean residence times (MRTs) in traps played historically a leading role [3,4,42–44] motivating a corresponding interpretation of the experimental data [45]. Some of the results of this approach can, however, be interpreted in a very different way, not assuming infinite MRTs [46], or even not assuming any moment of the residence time distribution (RTD) be infinite [6,7]. It is a much more physical vista on anomalous diffusion processes.

It seems obvious that both viscoelasticity and randomness are important ingredients of subdiffusion in such complex soft media. To combine viscoelasticity and randomness, several different approaches were developed, such as subordination of FBM to a CTRW [37], FBM on fractal structures [47,48], FBM with a subdiffusion coefficient randomly fluctuating in time [49,50], and GLE subdiffusion in random potentials [51,52]. The latter approach appeals by its generality and extensibility beyond thermal equilibrium [10,53,54]. It leads to several remarkable features, which we will show below are observed experimentally indeed. For this, we will look anew at the experimental data from several remarkable studies, which opted for different theoretical interpretations, and provide their alternative fits based on the theory of Langevin diffusion [6,7,55,56] and GLE subdiffusion [51,52] in random Gaussian landscapes. It will be shown that the approach of viscoelastic subdiffusion in random environments allows for a better understanding of previous experimental findings indeed.

II. SUBDIFFUSION IN SOME EXPERIMENTAL SYSTEMS REVISED

A. Water solutions of semiflexible actin filaments

Our first example relates to the water solutions of semiflexible actin filaments, an important model for cytosol [20]. On a macroscopic scale such media are viscoelastic and characterized by a complex shear modulus [12–14] $G^*(\omega) = G'(\omega) + iG''(\omega)$, with a power-law scaling, $G'(\omega), G''(\omega) \propto \omega^\alpha$, $\alpha \sim$ 0.5–0.85, in a frequency range $[\omega_{min}, \omega_{max}]$. The exponent α corresponds to power-law scaling in subdiffusion [12–14], $\langle \delta x^2(t) \rangle \propto t^\alpha$, which is observed in the time range $[t_{min}, t_{max}]$ with $t_{min} \sim 1/\omega_{max}$ and $t_{max} \sim 1/\omega_{min}$ [12–14,29]. However, the microscale properties of this subdiffusion can dramatically change depending on the ratio of the test particle's radius R to the averaged mesh size ξ of random actin meshwork [27–29]. Moreover, these properties also crucially depend [29] on a mean length of actin filaments L. Indeed, if $L \lesssim R$, the

particle feels such a medium as nearly homogeneous and exhibits a subdiffusion with macroscopic exponent α [see, e.g. experimental results for $L = 0.5$ μm and $R = 0.42$ μm in Fig. 1(a) of [29], where $\alpha \approx 0.85$ from $t_{min} \sim 0.5$ ms until about $t_{max} \sim 20$ s]. Notice that the results of the single-particle and two-particle microrheologies remarkably agree in such a case [29]. With increasing $L \gg R$, the two-particle microrheology probes subdiffusion on a macroscopic spatial scale [14,27,29,57] with α changed to $\alpha = 0.5$–0.75 [depending on L, see in Figs. 1(b)–1(d) of [29]]. The value $\alpha = 0.75$ corresponds to macroscopic shear modulus $G^*(\omega)$. The results of single-particle microrheology are, however, profoundly different [14,27,29,57], as it corresponds to particles feeling local cages of size ξ. Indeed, for $R > 1.5\xi$, the particles become practically trapped in the long-time limit [28], which is clearly seen in Fig. 1(b) of [29], where $\xi = 0.3$ μm and $L = 2$ μm. However, when a particle diffuses within a cage, it displays a subdiffusion with a macroscopic, nonobstructed value $\alpha = 0.75$, which agrees with the picture of locally viscoelastic subdiffusion in a random environment [52]. Accordingly, for $R \lesssim \xi$, on a large timescale, particles display a subdiffusion with $\alpha(t)$, which depends on the ratio R/ξ [28] and time.

1. Power-law subdiffusion

In Ref. [28], experimental data were fitted by a simple power-law dependence $\langle \delta x^2(t) \rangle = 2D_\alpha t^\alpha$ with a single time-independent exponent α and some anomalous diffusion constant D_α. It has obviously two fitting parameters α and D_α, with α related to a power-law scaling exponent of the residence time distribution $\psi(\tau) = c_\alpha/\tau^{1+\alpha}$ [4,11], at $\tau > \tau_0$, where τ_0 is a short-time cutoff required for normalization of $\psi(\tau)$. It has two fitting parameters, α and c_α. In our Fig. 1, we reexamine this interpretation. In parts (a) and (b) we plot the data extracted from Fig. 1 of [28] for $R = 0.25$ μm and various ξ. Generally, we see in part (a) that at least two values of α are required for different times. For $\xi = 0.75$ μm, $\alpha(t) \approx 1$ (upper dashed black line) until 0.2 s, i.e., diffusion is normal initially. Subsequently, it is, however, anomalously slow with $\alpha = 0.75$ (upper solid magenta line). With increasing R/ξ, an effective single α decreases; see in Fig. 2, where we fit the data extracted from Fig. 4 of [28] by $\alpha = 1/[1 + (1.45R/\xi)^4]$ dependence. For example, for $\xi = 0.55$ μm in Fig. 1(a), α becomes smaller. However, also in this case two α values, $\alpha \approx 0.825$ initially (dash-dotted blue line) and $\alpha \approx 0.596$ (dashed orange line) for large times, are needed to describe the experimental data consistently. Also for $\xi = 0.30$ μm and $\xi = R = 0.25$ μm, the power law fits with $\alpha \approx 0.344$ (lower solid light-green line) and $\alpha \approx 0.159$ (lower dashed red line), respectively, are not perfect.

Let us now look at the same data from a different perspective.

2. Sinai-like subdiffusion

Remarkably, the same data can alternatively be fitted by a Sinai-like power-of-logarithm dependence

$$\langle \delta x^2(t) \rangle = \xi^2 |\ln(t/t_0)/\sigma_{eff}|^a \tag{1}$$

with a in the range [2,4], and two other fitting parameters t_0 and σ_{eff} [see in Fig. 1(b)]. Such a dependence with $a = 4$
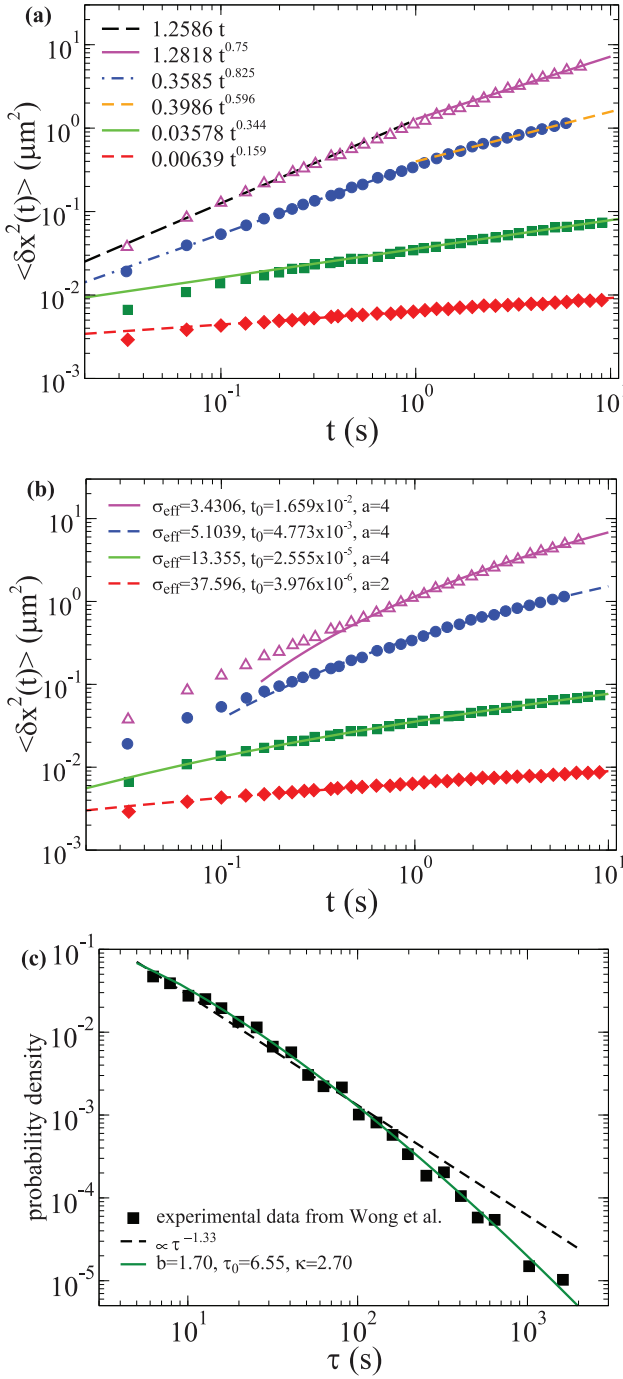
FIG. 1. Experimental data extracted using Engauge Digitizer [58] from Ref. [28] and their fits. In (a) and (b), the ensemble-averaged mean-square displacement vs time is taken from Fig. 1 in [28]. In all cases, $R = 0.25\ \mu$m; however, mesh size varies from $\xi = 0.75\ \mu$m (empty magenta triangles), through $\xi = 0.55\ \mu$m (filled blue circles) and $\xi = 0.30\ \mu$m (filled green squares) to $\xi = 0.25\ \mu$m (filled red diamonds). In (a), various power-law fits are presented with the parameters given in this plot (see the main text for more detail). In (b), the same data are fitted with Eq. (1) and the parameters shown. In (c), the data on the RTD from Fig. 3(b) of [28] for $\xi = 0.31\ \mu$m and the same R are fitted by (i) power-law dependence $\psi(\tau) \propto \tau^{-1-\alpha}$ with $\alpha = 0.33$, which was used in [28] (dashed black line), and (ii) a generalized log-normal distribution (2) (solid green line), with the parameters given in the plot.
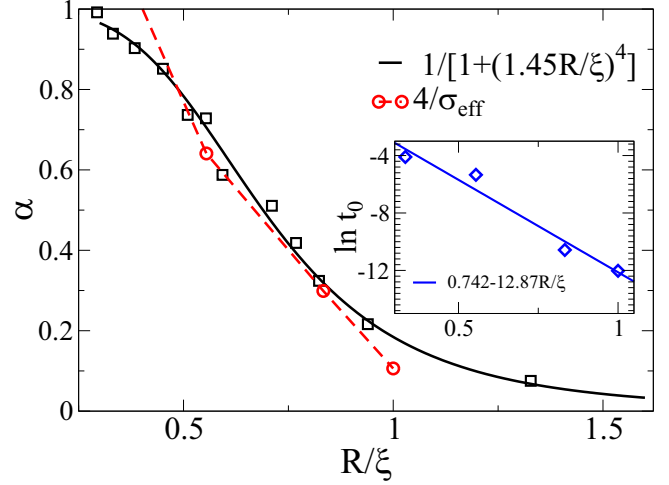

FIG. 2. Experimental data (empty black squares) on the dependence of subdiffusion exponent α on the ratio of the particle radius R and the mesh size ξ in an entangled actin meshwork and their fit (solid black line). Data are extracted using Engauge Digitizer [58] from Fig. 4 of Ref. [28]. Fit is done by $\alpha = 1/[1 + (cR/\xi)^d]$ dependence using one fitting parameter c at fixed $d = 4$. The optimal value is $c = 1.45$. The quality of fit is not visibly improved, if to make also d variable. The red open circles with their connecting dashed red line depict the value of $\alpha \approx 4/\sigma_{\text{eff}}$ predicted by our theory using fitting values σ_{eff} from Fig. 1(b), which in turn were obtained by applying Eq. (1) to data from Ref. [28]. The predicted value of α, which corresponds to $R/\xi = 1/3$, lies outside of the figure's frame, being unphysical, as α cannot exceed 1. This fit is expected to work only for $\sigma \gtrsim 2$ or $\sigma_{\text{eff}} \gtrsim 5.86$. Nevertheless, the overall agreement between the theory and experimental data is convincing. The inset shows fitting values t_0 from Fig. 1(b) and their exponential fit.

is known under the label of "Sinai-diffusion," and is widely considered as ultraslow diffusion [2,3], which can be a quite misleading naming [7]. By a simple scaling argumentation, like one used in [2], Eq. (1) was derived [7] for a memoryless diffusion in stationary zero-mean correlated Gaussian potentials $U(x)$, with the root-mean-square (rms) amplitude of fluctuations $\sigma = \langle \delta U^2(x) \rangle^{1/2}$ exceeding strongly thermal energy $k_B T$, $\sigma \gtrsim 5$, scaled in $k_B T$. It has two limiting theoretical values $a = 4$ and $a = 2$, which are related by $a = 2/\delta$ to the scaling law of the maximal amplitude of the potential fluctuation growth with distance, $|\delta U_{\max}(x)| \propto |\ln(x/x_{\text{in}})|^\delta$. Here, x_{in} depends on the functional form of correlation decay [7]. For a smooth disorder (e.g., with a Gaussian or power-law decay of correlations), it is defined by a spatial scaling parameter entering x dependence of the $\langle U(x_0)U(x_0 + x) \rangle$ correlations multiplied with some constant of the order of unity, which depends on the functional form of correlations [7]. Moreover, there is about one potential well per correlation length parameter for such a smooth disorder [7,52]. For these reasons, we identified x_{in} with ξ in Eq. (1). Notice, however, that ξ and σ_{eff} therein can be combined in one parameter, $\xi^2/\sigma_{\text{eff}}^a$. Furthermore, for any stationary Gaussian potential, $\delta = 1/2$ asymptotically [7], which yields $a = 4$, and $\sigma_{\text{eff}} = 2\sqrt{2}\sigma \approx 2.83\sigma$, in a semiquantitative agreement with numerics [7].

The occurrence of this Sinai-like diffusion was also shown for GLE subdiffusion in such random potentials [51,52].

Moreover, the theory [7] predicts that for a large σ, a can transiently be smaller, $a = 2$, due to transient features of $\delta U(x)$ fluctuations. The same transient features predict, in agreement with numerics [7] for $\sigma \gtrsim 2$, the emergence of a more common power-law dependence with $\alpha \sim 2/\bar{\sigma}_{\text{eff}} \approx$ const for several transient time decades, where $\bar{\sigma}_{\text{eff}} \sim \sigma_{\text{eff}}/2 = \sqrt{2}\sigma$. In numerical simulations, $\bar{\sigma}_{\text{eff}} \sim (1.24\text{--}1.52)\sigma$, depending on the disorder correlation features [6,7,51]. For viscoelastic subdiffusion in random Gaussian potentials, this estimate also works pretty well, e.g., for $\sigma = 4$ and $\sigma = 5$ [51,52]. Interestingly, a very similar dependence with $\alpha = 1/\sigma$, $0 < \alpha < 1$, also features CTRW with exponential energy disorder, power-law RTD $\psi(\tau) \propto 1/\tau^{1+\alpha}$, and diverging MRT [4,42–44].

In Fig. 1(b), larger R/ξ corresponds to larger σ_{eff} and smaller t_0, which can be fitted by $t_0 \approx \exp(0.742 - \Delta S/k_B)$, with $\Delta S/k_B \approx 12.97R/\xi$ (see inset in Fig. 2). The rationale behind this fit is that the attempt frequency $\nu_0 = 1/t_0$ to escape a cage depends exponentially on the entropic part ΔS of the free energy barrier, which depends on R/ξ. For $\sigma < 2$, the fit with Eq. (1) is not expected to be good. Nevertheless, it is not worse in part (b) than in part (a) of Fig. 1 for $\xi = 0.75 \ \mu$m (upper solid magenta line) and $\xi = 0.55 \ \mu$m (upper dashed blue line) and a sufficiently large t. For $\xi = 0.30 \ \mu$m (lower solid light-green line) and the fitting value $\sigma \approx 4.77$ it becomes much better than in (a). The fit for $\xi = 0.25 \ \mu$m (lower dashed red line) is also good. However, it requires a different $a = 2$. Importantly, the α values derived from such a simple theory agree well with the experimental values in Fig. 4 of [28] (see in Fig. 2).

All in all, our Eq. (1) does not have more free fitting parameters than the earlier fit of the same experimental data. Hence, the clear improvement of the fit quality is not due to an increased number of fitting parameters.

3. Residence time distributions

The case $\xi = 0.30 \ \mu$m is especially interesting because [28] provides an experimental RTD and its power law fit for the same R and similar $\xi = 0.31 \ \mu$m in Fig. 3 of [28]. We present this extracted experimental data and its fits in our Fig. 1(c). The power law with $\alpha = 0.33$ (dashed black line) fits the data over one time decade and correlates well with the diffusional exponents $\alpha = 0.32$ in [28] and $\alpha \approx 0.34$ in our Fig. 1(a). However, as was observed in [51], viscoelastic subdiffusion in a random Gaussian potential with $\sigma = 5$ and exponentially decaying correlations also yields $\alpha \approx 0.32$ and a generalized log-normal RTD [7,51]

$$\psi(\tau) \propto e^{-|\ln(\tau/\tau_0)/\kappa|^b}/\tau \qquad (2)$$

for $\tau \geqslant \tau_0$, with $b = 1.58$ and $\kappa = 3.33$. This RTD has also a power-law-looking part with $\alpha \approx 0.30$ [see Figs. 5(a) and 5(c) in [51] and the corresponding discussion. In Fig. 1(c) we make this statement more precise. Indeed, RTD (2) with $b = 1.7$ and $\kappa = 2.70$ (solid green line) fits the experimental points much better than a power-law distribution, if to relax the restriction $\tau \geqslant \tau_0$ [compare with Eq. (17) in [51] suitable in 1D]. It comes through all the experimental data points (with small error bars imagined). The RTD (2) has not only the first moment, but all the moments finite, which is typical for viscoelastic subdiffusion [10,59].

It should be mentioned that Eq. (2) has three fitting parameters, one more than a power-law distribution of infinite time range. However, can the major assumption on infinite MRT central for power-law fitting be justified from experimental data, in the considered case? Of course, in any experiment there are some minimal, $\tau_{\min}$, and maximal, $\tau_{\max}$, residence time intervals measured. This makes the corresponding conditional MRT

$$\langle\tau\rangle_c = \frac{1}{1-\alpha} \frac{\tau_{\max}^{1-\alpha} - \tau_{\min}^{1-\alpha}}{\tau_{\min}^{-\alpha} - \tau_{\max}^{-\alpha}} \qquad (3)$$

always finite. However, it increases and eventually diverges with increasing $\tau_{\max}$ as $\langle\tau\rangle_c \propto \tau_{\max}^{1-\alpha}$. So must do also the experimentally observed $\langle\tau\rangle_e$, which anyway should not be much smaller than $\tau_{\max}$. At odds with this, for experimental data in Fig. 1(c), we find $\langle\tau\rangle_e \approx 80.77$ s, while $\tau_{\max} \approx 1618$ s is about 20 times larger, and Eq. (3) yields $\langle\tau\rangle_c \approx 448.21$ s, also much larger than $\langle\tau\rangle_e$. In the discussed cases, the assumption of diverging MRT, upon increasing $\tau_{\max}$, is questionable indeed. The fact that Eq. (2) much better fits the experimental data cannot be attributed merely to one more parameter it uses.

Unfortunately, unlike in the CTRW theory based on power-law distributions, there is not at present a well-established relation between the parameters σ_{eff} or σ and t_0 in Eq. (1) and b, τ_0, and κ in Eq. (2). Some qualitative relations, however, exist. In particular, the larger σ, the smaller is $b \geqslant 1$ in Eq. (2). For example, for Gaussian disorder with power-law decaying correlations and $\sigma = 5$ in Fig. 5(b) of Ref. [51], $b = 1.88$ and $\kappa = 2.18$. For $\sigma = 2$ in the same figure, $b = 2.23$ and $\kappa = 1.43$. The parameter b also depends on the functional form of the correlations' decay. For example, for exponentially decaying correlations and $\sigma = 5$ in Fig. 5(a) of Ref. [51], $b = 1.58$ and $\kappa = 3.33$. In Fig. 1(c) here, $b = 1.7$ and $\kappa = 2.7$ with $\sigma = 4.77$, which interpolates between the values b and κ in the cases exponential and power-law decays in [51] for a similar $\sigma = 5$. Hence, a qualitative agreement is present.

B. Ion channels in biological membranes

Our second example relates to subdiffusion of Kv2.1 potassium ion channel proteins clustered in biological membranes, which was investigated in [48]. Experimental RTD distributions extracted from Fig. 4 of this paper are shown in Fig. 3 for two sizes of the initial confinement area with radius R_H. A power-law fit with $\alpha = 0.9$ [48] (dashed red line) covers at most one time decade with a significant data scatter due to poor statistics. For the smaller R_H statistics is improved. However, the largest residence time in this case does not exceed 4 s. Hence, the tail of distribution decays obviously faster than the claimed power law. Our generalized log-normal fit (dash-dotted light-green and solid black lines) to the same data with Eq. (2) is much better. In both cases, $b = 1.91$ and $b = 1.92$, correspondingly, are rather close to log-normal $b = 2$. Moreover, the values κ are also similar for two values of R_H. Clearly what makes a difference is the value of τ_0, which is essentially smaller for smaller R_H. This provides clear evidence that the MRT is not only finite, but it also diminishes with R_H. Indeed, in this figure, $\langle\tau\rangle_e \approx 0.77$ s for the experimental data point at $R_H = 44.72$ nm, whereas the corresponding $\tau_{\max} \approx 9$ s. Also for $R_H = 22.36$ nm in this
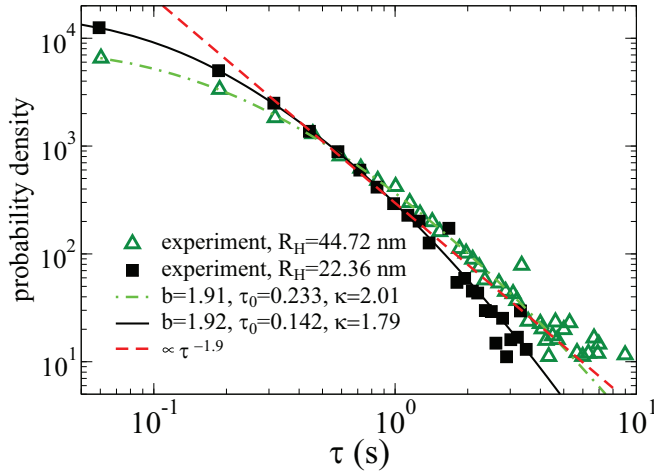
FIG. 3. Experimental RTD and their fits. Data for two values $R_H \approx 22.36$ nm (filled black squares) and $R_H \approx 44.72$ nm (empty green triangles) are extracted using Engauge Digitizer [58] from Fig. 4 in [48] for clustered Kv2.1 ion channels initially confined to a circle of radius R_H. Different fits are presented: (i) power law with $\alpha = 0.9$ (dashed red line) following [48], for $R_H \approx 22.36$ nm; (ii) generalized log-normal distributions (2) (dash-dotted light-green and solid black lines), with the parameters shown. The second fit is evidently better than the power-law fit, which covers one time decade at best and is hampered by a strong data noise for $\tau > 4$ s. Moreover, for $R_H \approx 22.36$ nm the RTD is most obviously not a power law asymptotically—the largest experimental residence time is about 4 s only.

figure, $\langle \tau \rangle_e \approx 0.355$ s for the experimental data points, whereas the corresponding $\tau_{\max} \approx 3.5$ s. From this, we conclude that $\langle \tau \rangle \propto R_H$ approximately, which is to be expected for finite mean residence times, independently of how large is $\tau_{\max}$.

Physically, the actin elements of cytoskeleton make also a random meshwork on the biological membranes creating pockets of a random size, where diffusing particles can be trapped. Hence, a physical picture of viscoelastic subdiffusion in a random potential is also relevant in this case. It is complementary to the approach of viscoelastic subdiffusion subordinated to a diffusion on fractal structures developed in [48]. In addition, diffusion of lipid molecules and proteins in crowded lipid-protein membranes without cytoskeleton elements [41,60,61] fits well into our concept, as discussed in [52], and possibly even diffusion of water molecules near lipid membranes [17], and drug molecules in interface water [18,19].

C. Subdiffusion of RNA-protein particles in cytosol

Finally, we revisit experimental results on distribution of RNA-protein particle subdiffusive displacements in cytosol of *Escherichia coli* and *Saccharomyces cerevisiae* cells [39] fitted therein by Laplace distribution $P(x,t) \propto \exp(-|x/x_1(t)|)$. It is a particular case, with $\chi = 1$, of the exponential power distribution (EPD)

$$P(x,t) \propto \exp(-|x/x_\chi(t)|^{\chi(t)}). \tag{4}$$

The Laplace or exponential distribution was earlier proposed in relation to anomalous yet Brownian diffusion in soft matter
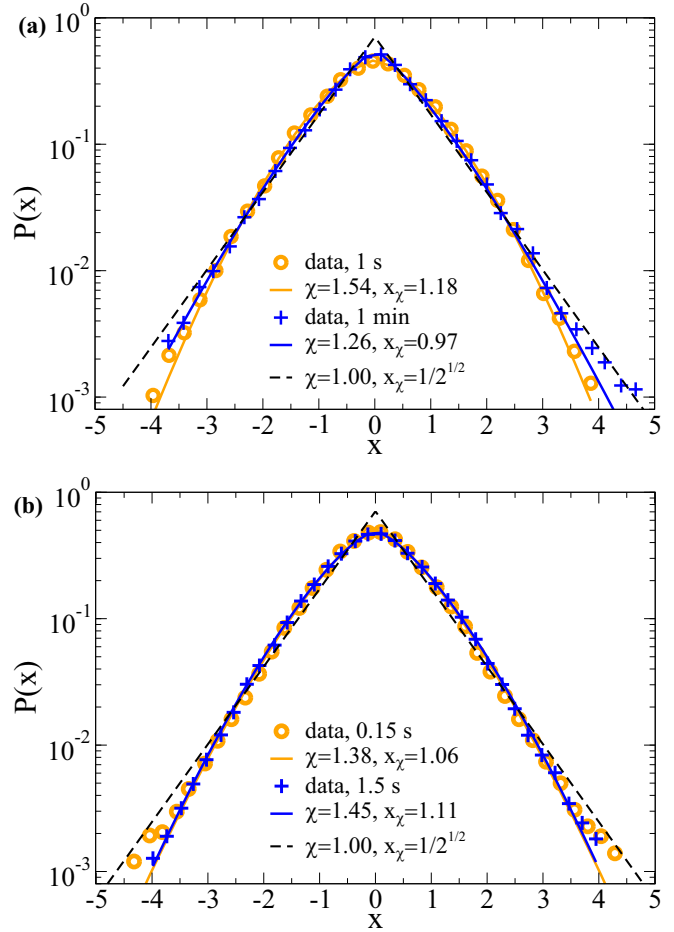

FIG. 4. Displacement distribution of RNA-protein particles in the cytosol of (a) *E. coli* cells and (b) *S. cerevisiae* cells normalized by the standard deviation of displacement for two instants of time in each case. Data are taken from Fig. 4 of [39] using Engauge Digitizer [58]. Fits [solid blue (dark) and orange (light) lines] are done using Eq. (4) with fitting parameters shown in the plots. Variable values $1 < \chi < 2$ allow for visibly better fits of the central part than the scaled and normalized Laplace distribution $P(x) = \exp(-\sqrt{2}|x|)/\sqrt{2}$ (dashed black lines) [39], also depicted for comparison.

including actin filament solutions [8,9]. We relax this restriction on χ and use (4) with a variable power χ. The results are depicted in Fig. 4(a) for *E. coli* and (b) for *S. cerevisiae* cells. The central part of the experimental distribution is clearly much better described by the EPD with $\chi \sim 1.26$–1.54.

Importantly, the distribution (4) also emerges for diffusion in random potentials [6], including viscoelastic GLE subdiffusion [52]. In addition, it appears for diffusion of lipids and proteins in crowded lipid-protein systems [41,60,61], and of drug molecules in interface water [19]. Importantly, the larger σ, the smaller is $\chi \geqslant 1$ in Eq. (4) within our model. For example, for $\sigma = 4$, in Fig. 2 of the Supplemental Material in Ref. [6], χ is about 1.37. It still did not reach its minimum, while evolving in time. In the same figure, χ is about 1.5 at the minimum for $\sigma = 2$. Likewise, for $\sigma = 2$ in Ref. [52], χ is about 1.59 at its minimum in Fig. 3(c) therein. For $\sigma = 4$, it is about 1.45 at the end of simulations, where the minimum was

not reached. For larger σ, χ is expected to be smaller. Hence, a qualitative agreement with the results in Fig. 4 of this paper is present.

In this respect, subdiffusion of mRNAs in *E. coli* revealed and studied first in [34] was initially interpreted as a CTRW subdiffusion because of a large scatter in single trajectory averages [45], which should not be the case of *ergodic* GLE viscoelastic subdiffusion in a homogeneous environment [59,62]. However, later on it was shown that this subdiffusion is, in essence, of viscoelastic FBM or GLE origin [63]. Likewise, patently viscoelastic subdiffusion in [15,39] exhibits a large scatter in single-trajectory averages. Some scatter can, of course, emerge because of the particles' different size [64]. However, it cannot be the only reason because the scatter can be large, several orders of magnitude, as characterized by the anomalous diffusion coefficient defined for single trajectories, and the particle size varies not that strongly. Also for viscoelastic subdiffusion in random environments, one of the fingerprints of is a broad scatter of single-trajectory time average of the particles' mean-square displacement [51,52]. It can be characterized by a pair (α, D_α) of power-law exponent α and the corresponding subdiffusion coefficient D_α, which are both broadly distributed [51,52]. The average single-trajectory α agrees, however, pretty well with α defined using the ensemble average. This picture agrees well with the experimental results in [15,39], where a similar phenomenon was observed and gave the grounds for the authors of [15,39] to claim that the diffusion they observed and studied is ergodic. In the theory developed in [39], one assumes, however, that α is not distributed, but only D_α has an exponential distribution. The latter leads to the Laplace, or exponential distribution with $\chi = 1$ in Eq. (4). However, if we relax the assumption of constant α, which in fact does not fully agree with the results presented in Figs. 1(c) and 1(d) of [39], then it is also natural to relax the assumption of constant $\chi = 1$. Indeed, variable χ results in a better agreement with experiment in our Fig. 4.

Viscoelastic subdiffusion in random environments provides a natural theoretical framework to reconcile viscoelasticity with nonergodic features caused by randomness [51,52]. It is an important message of this work.

III. DISCUSSION AND CONCLUSIONS

We wish to underline that our concept does not contradict other suggestions to combine viscoelastic FBM and GLE features with breaking ergodicity. Rather, it provides a unifying framework. Indeed, local subdiffusion in random-size pockets of complex meshworks can phenomenologically be characterized by a local random pocket-specific subdiffusion coefficient. It can be interpreted as an inhomogeneous viscoelastic subdiffusion with a randomly distributed subdiffusion coefficient as is done in [38,39], if on the observation timescale the particles do not change their localization pocket. It can also be the reason why diffusion can be seen normal from the perspective of the single-trajectory averages and anomalous on the ensemble level [40], even if it can be modeled differently, with a fluctuating in time diffusion [40] or subdiffusion [49,50] coefficient.

However, when the particles jump to other localization pockets on the observation timescale, like in [28] (see Fig. 2

therein), then a CTRW picture might seem more appropriate, and it was taken in [28]. Viscoelastic subdiffusion in random environments provides a general theoretical framework to unify different perspectives. It provides a natural extension and generalization of a random landscape approach to anomalous diffusion [2] practiced for many years assuming local diffusion be normal. In this respect, we wish to observe that the initial time in Fig. 1 here and in [28] starts from about 0.03 s. However, if one were to extend it down to 0.1 ms, like in [29], then the regime of initial subdiffusion with $\alpha = 0.75$ until 0.01 s matching the macroscopic behavior becomes obvious [see parts (b)–(d) in Fig. 1 of [29]], even if asymptotically particles become practically trapped at $R/\xi = 1.4$ with the asymptotic value of α smaller than 0.1. Also in Fig. 1(a) of Ref. [57], the results of two-particle microrheology (the lower curve therein), which probes the diffusion behavior on a macroscale, implicate subdiffusion with bulk value $\alpha = 0.75$. However, the results of single-particle microrheology (the upper curve therein) indicate clearly a subdiffusion of Sinai-like type, our Eq. (1), which is caused by local environment. It agrees well with a general picture of a finite-range viscoelastic subdiffusion in a random environment [52]. Noteworthy, judging from the minimal $\omega_{\min}$ of power-law scaling of $G^*(\omega)$ in actin solutions, the macroscopic scale subdiffusion in Ref. [29] should not extend beyond the temporal range of 10–20 s. However, subdiffusion caused by trapping in random pockets of actin meshwork for the particle size R comparable with the mesh size ξ can extend far beyond this range, as our theory predicts generally [52]. It is an experimentally verifiable prediction, which seems to be in line with the experimental results in [29,57].

To conclude, it is amazing that the functional dependencies (1)–(4) emerged within the studies of one-dimensional GLE viscoelastic subdiffusion in stationary Gaussian potentials [51,52]—a theoretical toy model—prove their importance while fitting the results obtained for real three-dimensional (3D) and two-dimensional (2D) viscoelastic disordered systems much better than the original fits based on different theories. This signifies our approach's validity and importance and calls for its further exploration and extension, particularly 2D and 3D, different random potentials (models of spatial disorder), and models of time correlations, including fluctuating in time random potentials and out-of-equilibrium effects. There is plenty of research space opening in theory. The experimental studies based on these recent insights will be crucial. Therefore, we wish to invite researchers to rethink their data in the light of GLE viscoelastic subdiffusion in random environments as a fundamental approach.

[1] E. Frey and K. Kroy, Ann. Phys. (Leipzig) **14**, 20 (2005).

[2] J.-P. Bouchaud and A. Georges, Phys. Rep. **195**, 127 (1990).

[3] D. ben Avraham and S. Havlin, *Diffusion and Reactions in Fractals and Disordered Systems* (Cambridge University Press, Cambridge, 2000).

[4] B. D. Hughes, *Random Walks and Random Environments* (Clarendon, Oxford, 1995).

[5] Y. G. Sinai, Theor. Prob. Appl. **27**, 256 (1982).

[6] I. Goychuk and V. O. Kharchenko, Phys. Rev. Lett. **113**, 100601 (2014).

[7] I. Goychuk, V. O. Kharchenko, and R. Metzler, Phys. Rev. E **96**, 052134 (2017).

[8] B. Wang, S. M. Anthony, S. C. Bae, and S. Granick, Proc. Natl. Acad. Sci. USA **106**, 15160 (2009).

[9] B. Wang, J. Kuo, S. C. Bae, and S. Granick, Nat. Mater. **11**, 481 (2009).

[10] I. Goychuk, Adv. Chem. Phys. **150**, 187 (2012).

[11] R. Metzler, J.-H. Jeon, A. G. Cherstvy, and E. Barkai, Phys. Chem. Chem. Phys. **16**, 24128 (2014).

[12] F. Amblard, A. C. Maggs, B. Yurke, A. N. Pargellis, and S. Leibler, Phys. Rev. Lett. **77**, 4470 (1996).

[13] T. G. Mason and D. A. Weitz, Phys. Rev. Lett. **74**, 1250 (1995).

[14] T. A. Waigh, Rep. Prog. Phys. **68**, 685 (2005).

[15] S. C. Weber, A. J. Spakowitz, and J. A. Theriot, Phys. Rev. Lett. **104**, 238102 (2010).

[16] G. Guigas, C. Kalla, and M. Weiss, Biophys. J. **93**, 316 (2007).

[17] E. Yamamoto, T. Akimoto, Y. Hirano, M. Yasui, and K. Yasuoka, Phys. Rev. E **87**, 052715 (2013).

[18] R. Sarfati and D. K. Schwartz, ACS Nano **14**, 3041 (2020).

[19] A. Díez Fernández, P. Charchar, A. G. Cherstvy, R. Metzler, and M. W. Finnis, Phys. Chem. Chem. Phys. **22**, 27955 (2020).

[20] R. Phillips, J. Kondev, J. Theriot, and H. G. Garcia, *Physical Biology of the Cell*, 2nd ed. (Garland Science, New York, 2013).

[21] R. H. Pritchard, Y. Y. Shery Huang, and E. M. Terentjev, Soft Matter **10**, 1864 (2014).

[22] P. Sollich, F. Lequeux, P. Hébraud, and M. E. Cates, Phys. Rev. Lett. **78**, 2020 (1997).

[23] B. Fabry, G. N. Maksym, J. P. Butler, M. Glogauer, D. Navajas, and J. J. Fredberg, Phys. Rev. Lett. **87**, 148102 (2001).

[24] D. Robert, T.-H. Nguyen, F. Gallet, and C. Wilhelm, PLoS One **5**, e10046 (2010).

[25] K. Kroy and J. Glaser, New J. Phys. **9**, 416 (2007).

[26] K. Kroy, Soft Matter **4**, 2323 (2008).

[27] M. L. Gardel, M. T. Valentine, J. C. Crocker, A. R. Bausch, and D. A. Weitz, Phys. Rev. Lett. **91**, 158302 (2003).

[28] I. Y. Wong, M. L. Gardel, D. R. Reichman, E. R. Weeks, M. T. Valentine, A. R. Bausch, and D. A. Weitz, Phys. Rev. Lett. **92**, 178101 (2004).

[29] J. Liu, M. L. Gardel, K. Kroy, E. Frey, B. D. Hoffman, J. C. Crocker, A. R. Bausch, and D. A. Weitz, Phys. Rev. Lett. **96**, 118104 (2006).

[30] K. Luby-Phelps, Mol. Biol. Cell **24**, 2593 (2013).

[31] M. J. Saxton and K. Jacobsen, Annu. Rev. Biophys. Biomol. Struct. **26**, 373 (1997).

[32] M. Weiss, M. Elsner, F. Kartberg, and T. Nilsson, Biophys. J. **87**, 3518 (2004).

[33] D. S. Banks and C. Fradin, Biophys. J. **89**, 2960 (2005).

[34] I. Golding and E. C. Cox, Phys. Rev. Lett. **96**, 098102 (2006).

[35] J. H. Jeon, V. Tejedor, S. Burov, E. Barkai, C. Selhuber-Unkel, K. Berg-Sørensen, L. Oddershede, and R. Metzler, Phys. Rev. Lett. **106**, 048103 (2011).

[36] F. Höfling and T. Franosch, Rep. Prog. Phys. **76**, 046602 (2013).

[37] S. M. A. Tabei, S. Burov, H. Y. Kima, A. Kuznetsov, T. Huynha, J. Jureller, L. H. Philipson, A. R. Dinner, and N. F. Scherer, Proc. Natl. Acad. Sci. USA **110**, 4911 (2013).

[38] W. He, H. Song, Y. Su, L. Geng, B. J. Ackerson, H. B. Peng, and P. Tong, Nat. Commun. **7**, 11701 (2016).

[39] T. J. Lampo, S. Stylianidou, M. P. Backlund, P. A. Wiggins, and A. J. Spakowitz, Biophys. J. **112**, 532 (2017).

[40] C. Manzo, J. A. Torreno-Pina, P. Massignan, G. J. Lapeyre, M. Lewenstein, and M. F. Garcia Parajo, Phys. Rev. X **5**, 011021 (2015).

[41] R. Metzler, J.-H. Jeon, and A. G. Cherstvy, Biochem. Biophys. Acta **1858**, 2451 (2016).

[42] M. F. Shlesinger, J. Stat. Phys. **10**, 421 (1974).

[43] H. Scher and E. W. Montroll, Phys. Rev. B **12**, 2455 (1975).

[44] R. Metzler and J. Klafter, Phys. Rep. **339**, 1 (2000).

[45] Y. He, S. Burov, R. Metzler, and E. Barkai, Phys. Rev. Lett. **101**, 058101 (2008).

[46] I. Goychuk, Phys. Rev. E **86**, 021113 (2012).

[47] Y. Meroz, I. M. Sokolov, and J. Klafter, Phys. Rev. E **81**, 010101(R) (2010).

[48] A. V. Weigel, B. Simon, M. M. Tamkun, and D. Krapf, Proc. Natl. Acad. Sci. USA **108**, 6438 (2011).

[49] A. Sabri, X. Xu, D. Krapf, and M. Weiss, Phys. Rev. Lett. **125**, 058101 (2020).

[50] W. Wang, F. Seno, I. M. Sokolov, A. V. Chechkin, and R. Metzler, New J. Phys. **22**, 083041 (2020).

[51] I. Goychuk, Phys. Chem. Chem. Phys. **20**, 24140 (2018).

[52] I. Goychuk and T. Pöschel, New J. Phys. **22**, 113018 (2020).

[53] I. Goychuk, Chem. Phys. **375**, 450 (2010).

[54] I. Goychuk, V. O. Kharchenko, and R. Metzler, PLoS One **9**, e91700 (2014).

[55] A. H. Romero and J. M. Sancho, Phys. Rev. E **58**, 2833 (1998).

[56] M. Khoury, A. M. Lacasta, J. M. Sancho, and K. Lindenberg, Phys. Rev. Lett. **106**, 090602 (2011).

[57] A. Sonn-Segev, A. Bernheim-Groswasser, H. Diamant, and Y. Roichman, Phys. Rev. Lett. **112**, 088301 (2014).

[58] M. Mitchell, B. Muftakhidinov, T. Winchen, Z. Jedrzejewski-Szmek, A. Trande, J. Weingrill, S. Langer, D. Lane, and K. Sower, Engauge Digitizer Software, http://markummitchell.github.io/engauge-digitizer/, 2019.

[59] I. Goychuk, Phys. Rev. E **80**, 046125 (2009).

[60] J.-H. Jeon, Hector Martinez-Sera Monne, M. Javanainen, and R. Metzler, Phys. Rev. Lett. **109**, 188103 (2012).

[61] J.-H. Jeon, M. Javanainen, H. Martinez-Seara, R. Metzler, and I. Vattulainen, Phys. Rev. X **6**, 021006 (2016).

[62] W. Deng and E. Barkai, Phys. Rev. E **79**, 011112 (2009).

[63] M. Magdziarz, A. Weron, K. Burnecki, and J. Klafter, Phys. Rev. Lett. **103**, 180602 (2009).

[64] J. Ślęzak, R. Metzler, and M. Magdziarz, New J. Phys. **20**, 023026 (2018).